Physica B 406 (2011) 3588–3591

Contents lists available at ScienceDirect

Physica B

journal homepage: www.elsevier.com/locate/physb

Down-conversion near infrared emission in Pr^{3+}, Yb^{3+} co-doped Y_2O_3 transparent ceramics

Guang-min Yang [a], Sheng-ming Zhou [b,*], Hui Lin [b,*], Hao Teng [b]

[a] College of Physics, Changchun Normal University, Changchun, Jilin Province 130000, China
[b] Key Laboratory of Materials for High Power Laser, Shanghai Institute of Optics and Fine Mechanics, Chinese Academy of Sciences, P.O. Box 800-211, Shanghai 201800, China

ARTICLE INFO

Article history:
Received 25 May 2011
Received in revised form
17 June 2011
Accepted 18 June 2011
Available online 24 June 2011

Keywords:
Transparent ceramics
Down-conversion
Near infrared emission
Energy transfer mechanisms
Crystalline silicon solar cells

ABSTRACT

Pr^{3+}, Yb^{3+} co-doped Y_2O_3 transparent ceramics have been prepared by the solid state reaction and vacuum sintering. Down-conversion near infrared emission has been demonstrated upon a 482 nm excitation. The energy of the 482 nm blue photon was first absorbed by Pr^{3+} and then delivered to Yb^{3+}. Possible energy transfer mechanisms from Pr^{3+} to Yb^{3+} have been discussed. Under the 482 nm excitation, the Pr^{4+}–Yb^{2+} charge transfer state would not seriously influence the energy transfer process. The dominant one should be either the cooperative down-conversion or the two-step photon emission. The efficient down-conversion near infrared emission has potential application in enhancing the conversion efficiency of crystalline silicon solar cells.

1. Introduction

Recently efficient down-conversion near-infrared (NIR) emission, that is, converting one UV or blue photon into two or more NIR photons was intensively studied. This efficient energy conversion process was also called "NIR quantum cutting" (NIR QC). Its promising potential application is to reduce the charge carrier thermalization in the present commercial crystalline silicon solar cells [1–4]. So far, the NIR QC process was achieved in different kinds of host materials (including powders [5–9], glasses [10,11], glass ceramics [12–17] and thin films [18]) by co-doping a donor ion like Tb^{3+}, Tm^{3+}, Pr^{3+}, Eu^{2+} or Ce^{3+}, and Yb^{3+} as the acceptor. Recently, the QC process in transparent ceramic materials has been reported in Refs. [19,20]. The advantages of transparent ceramic hosts lie in their high transparency and their good physical, chemical and ultraviolet radio-resistance stability. Among the different kinds of transparent ceramic materials, Y_2O_3 is a commonly investigated one. The benefits of the Y_2O_3 host are its high thermal conductivity for efficient thermal load removal, high transparency from ultraviolet to mid-infrared, good physical and chemical stability and its low phonon energy among the oxide materials. [21] So here in this paper we report the down-conversion NIR emission in Pr^{3+}, Yb^{3+} co-doped Y_2O_3 transparent ceramics. The energy transfer mechanisms from Pr^{3+} to Yb^{3+} in the Y_2O_3 host under the 482 nm excitation were discussed.

2. Experimental

Firstly, Pr_6O_{11} (99.999%), Yb_2O_3 (99.999%) and Y_2O_3 (99.999%) powders according to the designed $(Pr_{0.01}Y_{0.99-x}Yb_x)_2O_3$ ($x=0$, 0.02, 0.05 and 0.1; named as P0, P1, YP2 and P3, respectively) fomula with 0.5wt% ethyl orthosilicate were mixed by ball milling in ethanol for 12 h. After drying, the powders were first uniaxially pressed into plates at 10 MPa and then cold isostatically pressed at 200 MPa. The plates were sintered at 1850 °C under a base pressure of $\sim 1.0\times10^{-3}$ Pa for 20 h. The as-sintered samples were annealed in the air at 1450 °C to eliminate the possible introduction of Yb^{2+} or O^{2-} vacancies during the vacuum sintering. Then every sample was double-side polished to 1 mm thickness (shown in Fig. 1). The optical transmittance and absorption spectra of the samples were measured on a V-570-type ultraviolet/visible/near-IR spectrophotometer (JASCO, Japan). JSM 6360-LA scanning electron microscopy (JEOL, Kyoto, Japan) was used to analyze the microstructure of ceramics. The excitation, emission spectra and the Pr^{3+} 511 nm emission decay curves were measured on an FLS920 fluorescence spectrometer (Edinburgh Instruments, Britain). All the characterizations were performed at room temperature.

3. Results and discussion

Fig. 1 presents a picture of the single Pr^{3+} doped, and the Pr^{3+}, Yb^{3+} co-doped Y_2O_3 transparent ceramic samples after double-side mirror polishing. The characters behind the samples could be

* Corresponding authors. Tel.: +86 21 69918482; fax: +86 21 69918607.
E-mail addresses: zhousm@siom.ac.cn (S. Zhou), linh8112@163.com (H. Lin).

0921-4526/$ - see front matter © 2011 Elsevier B.V. All rights reserved.
doi:10.1016/j.physb.2011.06.044

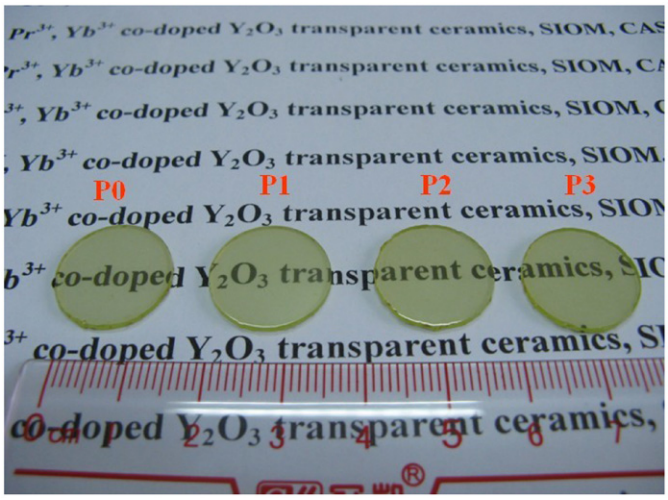

Fig. 1. Picture of the Pr^{3+}, Yb^{3+} co-doped Y_2O_3 ceramic samples.

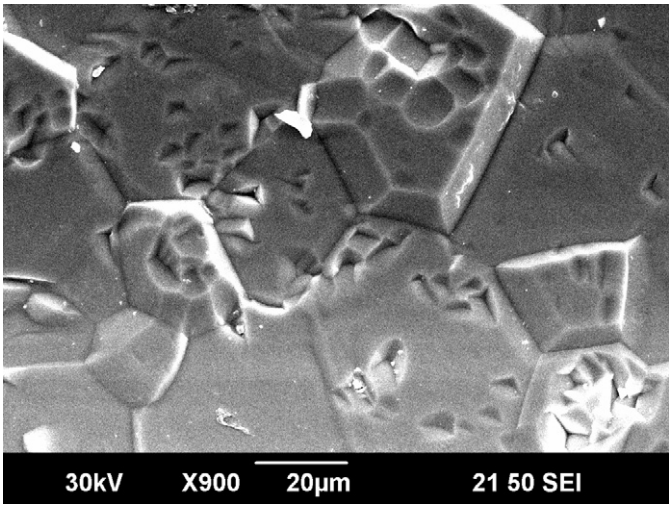

Fig. 3. SEM morphology of the microstructure of Sample P0.

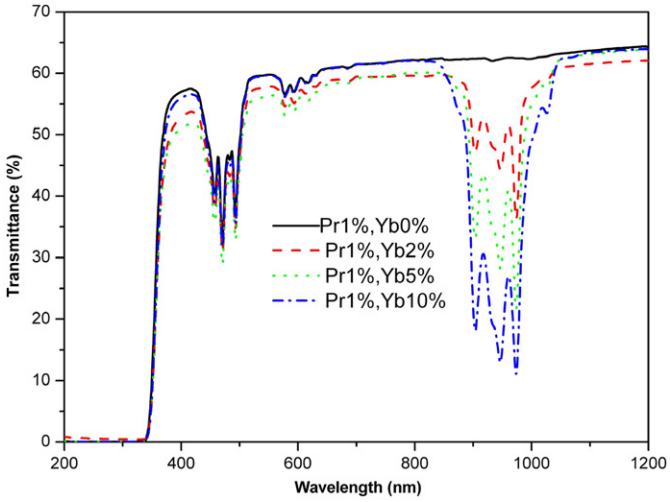

Fig. 2. Optical transmittance of the Pr^{3+}, Yb^{3+} co-doped Y_2O_3 transparent ceramics.

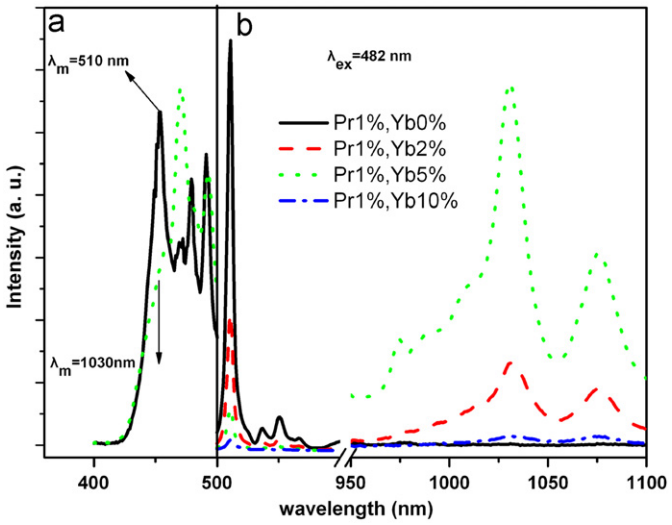

Fig. 4. (a) Solid line: excitation spectrum of Sample P0, λ_{em}=511 nm; dotted line: excitation spectrum of Sample P2, λ_{em}=1030 nm; (b) emission spectra of the four transparent ceramic samples, λ_{ex}=482 nm.

clearly seen. X-ray diffraction θ–2θ scans (not given here) show that all the four samples were of the cubic Y_2O_3 structure (JCPDS41-1105).

Fig. 2 shows the transmittance of the four transparent ceramic samples. For P0 only the Pr^{3+}: $^3H_4 \rightarrow {}^3P_2$, $^3P_1+{}^1I_6$ transitions could be seen at 457, 470 and 493 nm [14], while for P1–P3, besides the absorption of Pr^{3+}, the Yb^{3+}: $^2F_{7/2} \rightarrow {}^2F_{5/2}$ transition between different Stark energy levels can be indentified around 1000 nm. The transmittance from 450 to 1200 nm for all the samples was $\geq$60% except for the absorption bands. The transparency of the ceramic samples could be further enhanced by optimizing the preparation process, for instance, to improve the temperature schedule, to select a proper sintering aid, etc.

The microstructures of ceramic samples were investigated by scanning electron microscopy (SEM). The SEM morphology of P0 is presented in Fig. 3. Pores could be observed in the grains. The average grain size of the samples was ~30 μm.

Excitation spectra of P0 and P2 were carried out to demonstrate the $Pr^{3+} \rightarrow Yb^{3+}$ ET process (see Fig. 4(a)). With the Yb^{3+} 1030 nm emission monitored, the excitation band from 400 to 500 nm for P2 is in good agreement with that for P0 by monitoring the Pr^{3+} 511 nm emission.

In the emission spectra (Fig. 4(b)), for the Pr^{3+} single doped sample P0, under the 482 nm excitation, emission due to the Pr^{3+}: $^3P_0 \rightarrow {}^3H_5$, $^3H_6$ and $^3F_{3,4}$ transitions could be observed. There was no emission detected in the 950–1100 nm range, while for P1, P2 and P3, besides the emission of Pr^{3+}, the Yb^{3+} emission around 950–1100 nm could also be observed. This clearly demonstrated the ET from Pr^{3+} to Yb^{3+}. The emission of Pr^{3+} turned weaker with higher Yb^{3+} concentration, while the Yb^{3+} emission intensity reached a maximum for P2. The weakest Yb^{3+} emission in P3 indicated that severe concentration quenching of Yb^{3+} occurred.

The decay curves of the Pr^{3+}: 511 nm emissions under the 482 nm excitation for all the samples exhibited a non-exponential characteristic, as shown in Fig. 5. The mean lifetime (τ_m) can be calculated by [13]

$$\tau_m = \int_{t_0}^{\infty} [I(t)/I_0]dt \quad (1)$$

Table 1 gives the lifetime of the Pr^{3+}: 511 nm emissions for P0–P3. The higher the Yb^{3+} doping concentration, the shorter the lifetime of Pr^{3+}: 511 nm emissions. Since the concentration of

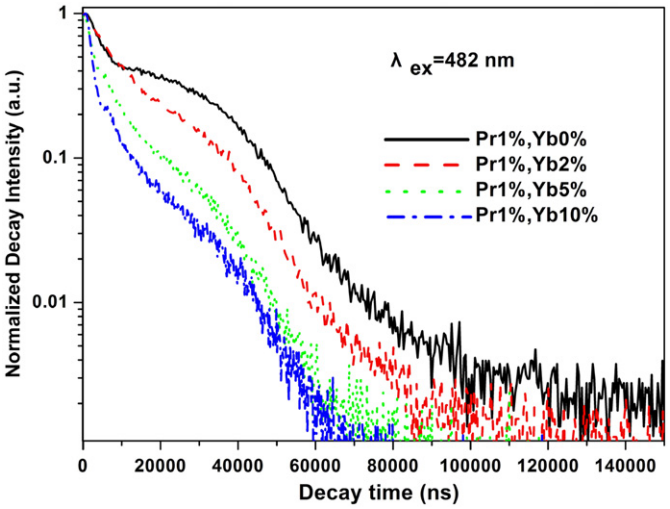

Fig. 5. Normalized decay curves of the Pr^{3+}: 511 nm emissions under the 482 nm excitation for the four transparent ceramic samples.

Table 1
Lifetime of the Pr^{3+} 511 nm emission and the $Pr^{3+}\rightarrow Yb^{3+}$ energy transfer efficiency (η_{ETE}) in Samples P0–P3.

Sample name	Lifetime of Pr^{3+} 511 nm emission (μs)	η_{ETE} (%)
P0 (x=0)	18.6	0
P1 (x=0.02)	14.6	21.5
P2 (x=0.05)	11.5	38.2
P3 (x=0.10)	6.3	–

Pr^{3+} was maintained constant in all the samples, the decrease of the Pr^{3+} 511 nm emission lifetime should not be attributed to the concentration quenching of Pr^{3+}. The $Pr^{3+}\rightarrow Yb^{3+}$ ET process can be a good reason for the decrease.

The energy transfer efficiency (η_{ETE}), defined as the ratio of the donors that are depopulated by the ET to the acceptors over the total number of donors being excited, has the following relationship with τ_m [13]:

$$\eta_{ETE} = 1 - \frac{\tau_{m-xYb}}{\tau_{m-0Yb}} \quad (2)$$

where τ_{m-0Yb} and τ_{m-xYb} stand for the mean lifetime of Pr^{3+} 511 nm emission for the Pr^{3+} single doped sample and the Pr^{3+}, Yb^{3+} co-doped samples with the Yb^{3+} concentration of x%, respectively. The calculated energy transfer efficiency for P1 and P2 is also given in Table 1. The maximum η_{ETE} from Pr^{3+} to Yb^{3+} is 38.2%.

Next, we will discuss the possible energy transfer mechanisms form Pr^{3+} to Yb^{3+} under the 482 nm excitation. First we can eliminate the influence of the Pr^{4+}–Yb^{2+} charge transfer state (CTS) in the ET process, denoted as "①" in Fig. 6. Generally, for some trivalent lanthanide ions like Pr^{3+}, Tb^{3+} and Ce^{3+}, tetravalent states tend to appear by loosing an electron while for Yb^{3+}, due to its $4f^{13}$ electron shell structure, Yb^{3+} tends to arrest an electron to the full f-shell structure. The CTS involved ET process is quite slow and will seriously quench the efficiency of Yb^{3+} emission [22]. However, under the 482 nm (the energy is quite low compared with that of deep ultraviolet or X-ray) excitation, the influence of CTS on the NIR down-conversion luminescence should be negligible. This should be attributed to the large energy gap between CTS and the Pr^{3+}:$^3P_0$ level, along with the low phonon energy of

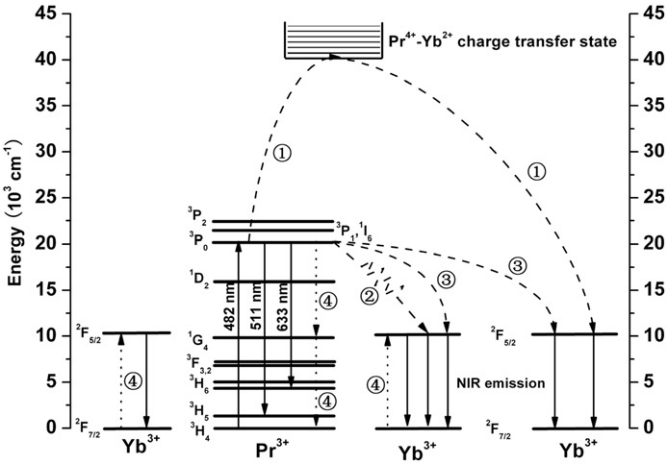

Fig. 6. Schematic energy level diagrams of Pr^{3+}, Yb^{3+} and the Pr^{4+}–Yb^{2+} charge transfer state illustrating the possible energy transfer mechanisms from Pr^{3+} to Yb^{3+} under the 482 nm excitation.

the Y_2O_3 host (max=~591 cm^{-1}) [23]. In addition the large energy gap between the Pr^{3+}:$^3P_0$ and Yb^{3+}:$^2F_{5/2}$ levels, together with the low phonon energy of Y_2O_3, makes the contribution of Pr^{3+}:$^3P_0 \xrightarrow{non\text{-}radiative}$ one Yb^{3+}:$^2F_{5/2} \xrightarrow{radiative} Yb^{3+}$:$^2F_{7/2}$ (denoted as "②" in Fig. 6) to the NIR emission negligible.

Since the Pr^{3+}:$^1G_4$ level is so close to the Yb^{3+}:$^2F_{5/2}$ level, which of the following competing ET processes played a dominant role was quite controversial. One was the second order process, namely the cooperative down-conversion from one Pr^{3+}:$^3P_0$ to the $^2F_{5/2}$ level of two Yb^{3+} ions [14], denoted as "③" in Fig. 6. It was believed that the Pr^{3+}:$^3P_0$+Yb^{3+}:$^2F_{5/2}\rightarrow Pr^{3+}$:$^1G_4$+$Yb^{3+}$:$^2F_{7/2}$ cross relaxation process would not counter much in the ET, for the Pr^{3+}:$^3P_0\rightarrow{}^1G_4$ transition possibility calculated from the Judd–Ofelt theory was very little. On the other hand, it was proposed recently that in the Pr^{3+}, Yb^{3+} co-doped $LiYF_4$ powders, the dominant ET process was the step photon emission, which was (1) firstly through the Pr^{3+}:$^3P_0$+Yb^{3+}:$^2F_{7/2}\rightarrow Pr^{3+}$:$^1G_4$+$Yb^{3+}$:$^2F_{5/2}$ cross relaxation, (2) and then followed by a resonant Pr^{3+}:$^1G_4\rightarrow Yb^{3+}$:$^2F_{5/2}$ ET and subsequent Yb^{3+}:$^2F_{5/2}\rightarrow Yb^{3+}$:$^2F_{7/2}$ emission, denoted as "④" in Fig. 6. Based on the Judd–Ofelt theory and Monte Carlo simulations combined with analytical calculation, it was argued that though the cross relaxation rate would be limited by the small oscillator strength of Pr^{3+}:$^3P_0\rightarrow{}^1G_4$ transition (<5%) [14,24], the cross relaxation step would still play a key role in the ET process due to the much higher (~10^3 times) possibility for its first order nature [24]. It should be pointed out that the NIR emission intensity was much stronger than that in the Tm^{3+}, Yb^{3+} co-doped Y_2O_3 transparent ceramics. We proposed that in Tm^{3+}, Yb^{3+} co-doped Y_2O_3, it was the cross relaxation that dominated the ET process. If cross relaxation also dominated the ET in Pr^{3+}, Yb^{3+} co-doped Y_2O_3, the relatively higher emission intensity should be attributed to the fact that Pr^{3+}:$^3P_0$+Yb^{3+}:$^2F_{7/2}\rightarrow Pr^{3+}$:$^1G_4$+$Yb^{3+}$:$^2F_{5/2}$ cross relaxation was almost free from the participation of phonons.

4. Conclusions

950–1100 nm NIR down-conversion emission has been achieved in Pr^{3+}, Yb^{3+} co-doped Y_2O_3 transparent ceramics. The NIR emission intensity was much stronger than the counterpart of the Tm^{3+}, Yb^{3+} co-doped Y_2O_3 transparent ceramics. This intense down-conversion NIR emission was either caused by the second order Pr^{3+}:$^3P_0\rightarrow 2Yb^{3+}$:$^2F_{5/2}$ cooperative down-conversion or the first order step photon emission free from the assistance of phonons.

Acknowledgement

This work was supported by the National Natural Science Foundation of China (no. 60990311) and the Key Basic Research Project of Science and Technology Committee of Shanghai (no. 10JC1415700). The authors would also like to express their sincere thanks to Mr. Ji-meng Cheng for his kind assistance in the excitation and emission spectra measurement.

References

[1] C. Strümpel, M. McCann, G. Beaucarne, V. Arkhipov, A. Slaoui, V. Švrček, C. del Cañizo, I. Tobias, Sol. Energy Mater. Sol. Cells 91 (2007) 238.
[2] T. Trupke, M.A. Green, P. Würfel, J. Appl. Phys. 92 (2002) 1668.
[3] B.S. Richards, Sol. Energy Mater. Sol. Cells 90 (2006) 1189.
[4] B.S. Richards, Sol. Energy Mater. Sol. Cells 90 (2006) 2329.
[5] P. Vergeer, T.J.H. Vlugt, M.H.F. Kox, M.I. DenHertog, J.P.J.M. van der Eerden, A. Meijerink, Phys. Rev. B 71 (2005) 014119.
[6] Q.Y. Zhang, C.H. Yang, Y.X. Pan, Appl. Phys. Lett. 90 (2007) 021107.
[7] Q.Y. Zhang, C.H. Yang, Z.H. Jiang, X.H. Ji, Appl. Phys. Lett. 90 (2007) 061914.
[8] Q.Y. Zhang, G.F. Yang, Z.H. Jiang, Appl. Phys. Lett. 91 (2007) 051903.
[9] L. Xie, Y. Wang, H. Zhang, Appl. Phys. Lett. 94 (2009) 061905.
[10] D. Chen, Y. Wang, Y. Yu, P. Huang, F. Weng, J. Appl. Phys. 104 (2008) 116105.
[11] X.F. Liu, Y.B. Qiao, G.P. Dong, S. Ye, B. Zhu, G. Lakshminarayana, D.P. Chen, J.R. Qiu, Opt. Lett. 33 (2008) 2858.
[12] S. Ye, B. Zhu, J. Luo, J. Chen, G. Lakshminarayana, J.R. Qiu, Opt. Express 16 (2008) 8989.
[13] S. Ye, B. Zhu, J. Chen, J. Luo, J.R. Qiu, Appl. Phys. Lett. 92 (2008) 141112.
[14] D. Chen, Y. Wang, Y. Yu, P. Huang, F. Weng, Opt. Lett. 33 (2008) 1884.
[15] D. Chen, Y. Wang, Y. Yu, P. Huang, F. Weng, J. Phys. Chem. C 113 (2009) 6406.
[16] D. Chen, Y. Yu, H. Lin, P. Huang, Z. Shan, Y. Wang, Opt. Lett. 35 (2010) 220.
[17] H. Lin, D. Chen, Y. Yu, A. Yang, Y. Wang, Opt. Lett. 36 (2011) 876.
[18] X.Y. Huang, Q.Y. Zhang, J. Appl. Phys. 105 (2009) 053521.
[19] H. Lin, S. Zhou, H. Teng, Y. Li, W. Li, X. Hou, T. Jia, J. Appl. Phys. 107 (2010) 043107.
[20] H. Lin, S. Zhou, X. Hou, W. Li, Y. Li, H. Teng, T. Jia, IEEE Photon. Technol. Lett. 22 (12) (2010) 866.
[21] K. Takaichi, H. Yagi, J. Lu, J.-F. Bisson, A. Shirakawa, K. Ueda, Appl. Phys. Lett. 84 (2004) 317.
[22] J. Ueda, S. Tanabe, J. Appl. Phys. 106 (2009) 043101.
[23] E. Husson, C. Proust, P. Gillet, J.P. Itié, Mater. Res. Bull. 34 (1999) 2085.
[24] J.T. van Wijngaarden, S. Scheidelaar, T.J.H. Vlugt, M.F. Reid, A. Meijerink, Phys. Rev. B 81 (2010) 155112.